This is a repository copy of *Interplay between Dopant Species and a Spin-Crossover Host Lattice during Light-Induced Excited-Spin-State Trapping Probed by Electron Paramagnetic Resonance Spectroscopy*.

White Rose Research Online URL for this paper:
http://eprints.whiterose.ac.uk/133041/

Version: Accepted Version

Interplay Between Dopant Species and a Spin-Crossover Host Lattice during Light-Induced Excited Spin-State Trapping Probed by EPR Spectroscopy

Sergey V. Tumanov,[†,‡] Sergey L. Veber,[†,‡] Sam Greatorex,[¶] Malcolm A. Halcrow*,[¶] and Matvey V. Fedin*,[†,‡].

[†]International Tomography Center SB RAS, Institutskaya str. 3a, 630090 Novosibirsk, Russia.

[‡]Novosibirsk State University, Pirogova str.2, 630090 Novosibirsk, Russia.

[¶]School of Chemistry, University of Leeds, Woodhouse Lane, Leeds LS2 9JT, UK.

ABSTRACT: Q-band Electron Paramagnetic Resonance (EPR) data conclusively demonstrate that the iron and cobalt centres in the solid solution $[Fe(bpp)_2]_{0.97}[Co(terpy)_2]_{0.03}[BF_4]_2$ (bpp = 2,6-di⟨pyrazol-1-yl⟩-pyridine) undergo allosteric spin state switching during light-induced excited spin state trapping (LIESST) at 20 K, and thermal relaxation around 80 K. EPR of $[Cu(terpy)_2]^{2+}$ and $[Cu(bpp)_2]^{2+}$, doped into the same host lattice, also indicates expansion of the copper coordination sphere during LIESST excitation.

Spin-crossover (SCO) compounds[1] continue to be heavily studied as components in multifunctional materials and nanostructures.[2,3] They are also useful testbeds for the development of new techniques and theories of molecular crystal engineering,[4] and more fundamental solid state physics.[5] SCO transitions can be induced at low temperatures by a number of stimuli, most commonly visible light.[6] That may lead to kinetic trapping of the sample in its excited spin state, the Light-Induced Excited Spin State Trapping (LIESST) effect.[1,7-9] Where relaxation by quantum mechanical tunnelling is slow, as in many iron(II) compounds, the sample only reverts to its ground state above a thermal activation temperature T(LIESST). This can be above 100 K in favourable cases.

Introduction of inert dopant ions into SCO materials affects their SCO cooperativity and temperature in predictable ways, without significantly changing the lattice structure.[9] Such studies have been important in the development of models for SCO processes,[10] and for understanding the dynamics of the LIESST experiment.[11] The use of dopant ions as spectroscopic probes of SCO is rarer, however. Most examples involve EPR of Mn^{2+} or high-spin Co^{2+} dopant ions, whose zero-field splitting is perturbed by SCO in the host-lattice.[12-19]

We have prepared solid solutions based on $[Fe(bpp)_2][BF_4]_2$ (bpp = 2,6-di⟨pyrazol-1-yl⟩pyridine),[20] which undergoes abrupt SCO at $T_{\frac{1}{2}}$ = 261 K and has useful LIESST properties with T(LIESST) = 81 K.[21,22] As well as the isomorphous metal dopants $[Fe_xM_{1-x}(bpp)_2][BF_4]_2$ (M = Co, Ni or Cu),[23-25] the same host lattice accommodates up to *ca* 25 % of $[M(terpy)_2]^{2+}$ (M = Co, Cu or Ru) dopants while remaining phase pure and apparently homogeneous.[23,25-27] Magnetic data suggested that SCO and the LIESST effect in $[Fe(bpp)_2]_y[Co(terpy)_2]_{1-y}[BF_4]_2$ (y = 0.85 or 0.76) involves switching at both the iron and cobalt centres. That repre-

sented the first example of allosteric switching of different metal ions in an SCO material; and, the first report of spin-state trapping in a solid cobalt(II) complex.[26,27] In comparison, the high-spin excited state of pure $[Co(terpy)_2][ClO_4]_2$ relaxes back to its low-spin ground state within 400 μs at 10 K in a LIESST-type experiment.[28]

The above conclusion remained tentative, however, since magnetic measurements cannot address the cobalt dopant ions directly. To address that limitation, we now report EPR studies of the LIESST effect in $[Fe(bpp)_2]_{0.97}[Co(terpy)_2]_{0.03}[BF_4]_2$ (**1**).[26] We also include similar measurements of two copper-doped analogues, $[Fe(bpp)_2]_{0.96}[Cu(terpy)_2]_{0.04}[BF_4]_2$ (**2**) and $[Fe_{0.97}Cu_{0.03}(bpp)_2][BF_4]_2$ (**3**),[25] since the Jahn-Teller (JT) structures of copper ions can be very sensitive to changes in their local environment.[13,14,29]

Chart 1. The complexes referred to in this work.

$[M(bpp)_2]^{2+}$
M = Fe or Cu

$[M(terpy)_2]^{2+}$
M = Co or Cu
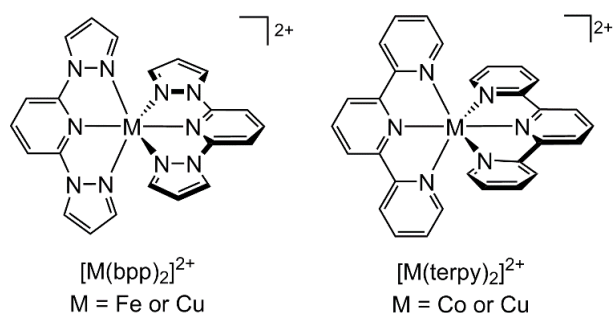
For this study, we employed high-resolution EPR at Q-band (34 GHz) to probe LIESST in compounds **1**-**3** using Co^{2+} or Cu^{2+} as reporters.[30] Suitable samples for photoswitching inside the EPR probe were prepared by dispersing the target compounds into KBr pellets, similar to routine FTIR preparations. The concentration of **1**-**3** was adjusted in each case as a tradeoff between sufficient transparency of the pellet and reasonable intensity of the EPR spectrum. Applying pressure to SCO-like compounds should be done with care, since sufficiently high pressures can modify their physico-chemical properties.[31] However, we ensured that polycrystalline powder samples and compounds dispersed in KBr pellets have very similar variable-temperature spectra (Figure S7). There-

fore, the impact of sample preparation on the SCO properties of **1-3** was insignificant.

All measurements were carried out using a Bruker Elexsys E580 EPR spectrometer at Q-band in continuous wave mode, while spectrum simulations were done using *EasySpin*.[32] Photoillumination was performed with a 532 nm OLED fed directly into the EPR probe by an optical fiber. As mentioned above, the host lattice $[Fe(bpp)_2][BF_4]_2$ undergoes LIESST at cryogenic temperatures with $T(LIESST) = 81$ K,[21] which is barely affected by the presence of <5 % dopant species, as in **1-3**.[23,26] Hence, the following experimental sequence was followed for each sample: the EPR spectrum was measured in the dark (prior to illumination) at $T = 20$ K; the sample was illuminated until no further spectral changes occurred, typically *ca* 10 mins; the photoswitched compound was warmed (in the dark) from 20 to 90 K, with spectra being measured at 10-20 K intervals; then, the sample was recooled to 20 K and remeasured, to compare the observed "relaxed" spectrum with the initial one. Each relaxed EPR spectrum at 20 K was identical to the one observed before illumination (Figures S2, S3 and S5).
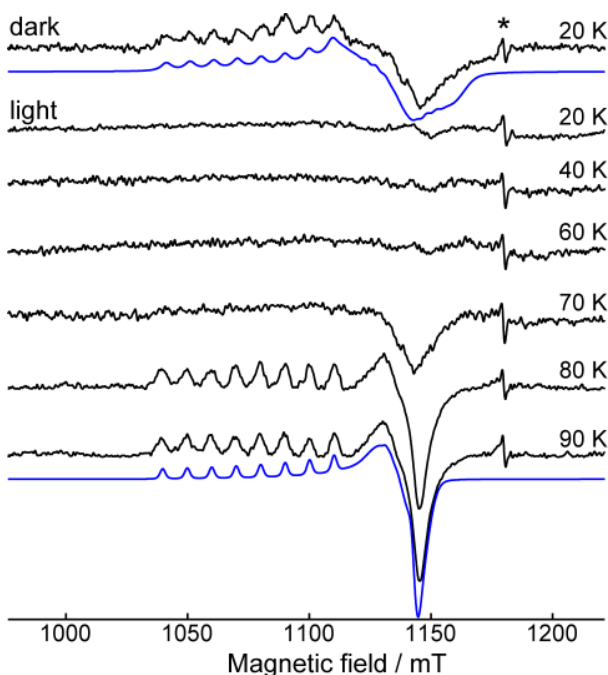

Figure 1. Q-band EPR spectra of powdered **1** dispersed in KBr. The sample was first measured prior to illumination (20 K, dark), then illuminated and remeasured (20 K, light). The temperature was then gradually increased and a series of spectra were recorded in the dark (40-90 K). Blue lines show simulations at 20 and 90 K. All spectra are normalized. The asterisk marks a radical impurity.

Fig. 1 shows the above series of measurements for **1**. The initial dark spectrum at 20 K is typical of low-spin ($S = 1/2$) Co^{2+} in a rhombically distorted octahedral environment. The 8 line hyperfine splitting due to the nuclear spin of ^{59}Co ($I = 7/2$) is clearly observed on the g_z component of the spectrum. The spectrum can be satisfactorily simulated using reasonable $g = [2.06\ 2.10\ 2.20]$ and hyperfine interaction $A_{zz} = 300$ MHz (≈107 G; A_{xx} and A_{yy} are not well resolved).[33] Upon photoillumination this spectrum disappears. Such change is unambiguously assigned to a conversion of low-spin Co^{2+} to its high-spin configuration ($S = 3/2$), whose EPR spectrum is much broader and less intense, being undetectable in our conditions.[25,34,35] As the temperature is increased, the EPR spectrum remains absent until the low-spin Co^{2+} signal reappears with a small fraction of its original intensity at 70 K, then regains

its full intensity at 80 K. This is consistent with the previously reported $T(LIESST)$ value of 80 K for **1**.[27] The spectroscopic parameters of the low-spin spectra at 80-90 K differ only slightly from those found at 20 K ($g = [2.068\ 2.088\ 2.201]$, $A_{zz} = 310$ MHz (≈110 G)), most likely due to a slight variation of the dopant molecular geometry with temperature and/or from dynamic Jahn-Teller (JT) effects.[34,36] To summarize, these data conclusively demonstrate that the $[Co(terpy)_2]^{2+}$ centers in **1** undergo quantitative, allosteric spin state switching during LIESST excitation and relaxation of the $[Fe(bpp)_2][BF_4]_2$ lattice. That is, the spin state of the $[Co(terpy)_2]^{2+}$ dopant is governed by the spin state of the iron(II) host material.

Fig. 2 shows a similar set of data for the $[Cu(terpy)_2]^{2+}$-doped analogue **2**. While some exchange-coupled copper(II)-nitroxyl clusters exhibit SCO-like phenomena,[1,37] magnetically isolated $3d^9$ Cu^{2+} species like $[Cu(terpy)_2]^{2+}$ cannot undergo SCO. However, the JT nature of this ion makes its EPR parameters, especially the *g*-tensor, highly sensitive to the small structural distortions imposed by surrounding lattice.
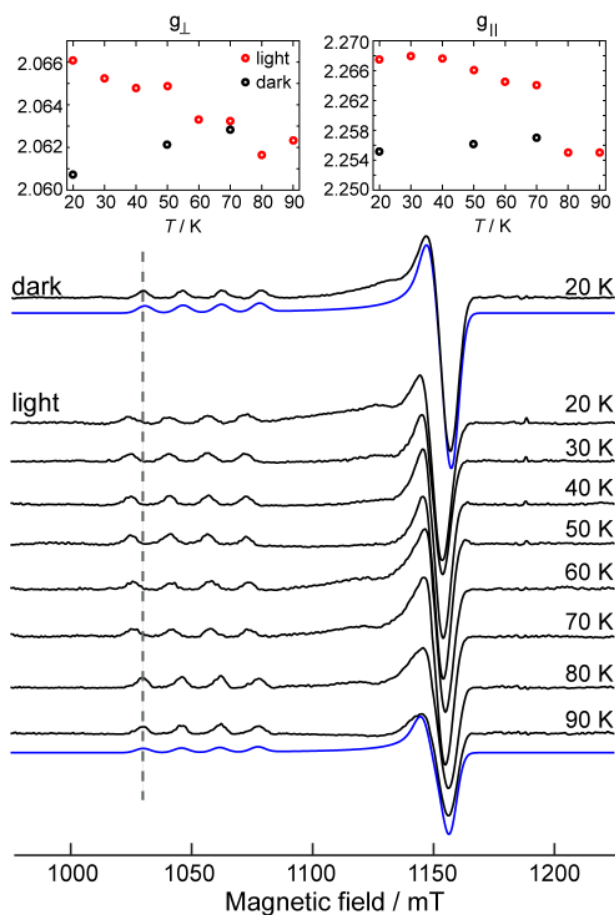
Figure 2. Q-band EPR spectra of powdered **2** dispersed in KBr. Details as in Figure 1. The dashed vertical line guides the eye to visualise the changes in $g_{\parallel}$ during the experiment. The upper insets show the temperature evolution of $g_{\perp}$ and $g_{\parallel}$ in the illuminated sample (red), and in the reference measurements on the same pellet without illumination (black; Figure S4).

The spectrum at 20 K before illumination is typical of Cu^{2+} in an axially symmetric octahedral environment (Fig. 2) and can be simulated using $g = [2.061\ 2.061\ 2.252]$. The photoswitching of the $[Fe(bpp)_2][BF_4]_2$ host lattice at 20 K is readily reflected in the change of the $g_{\parallel}$ (g_z) and $g_{\perp}$ ($g_{x,y}$) components of the tensor. Nota-

bly all components of the g-tensor, and thus its isotropic value, increase upon low→high-spin photoconversion of Fe^{2+} lattice, to g = [2.066 2.066 2.268] at 20 K. Such changes likely correspond to a lengthening of the Cu–N bonds, meaning that the effective volume of CuN_6 coordination octahedron has expanded. This is reasonable, since LIESST excitation in $[Fe(bpp)_2][BF_4]_2$ leads to a 2 % isothermal increase in its unit cell volume, reflecting the longer metal–ligand bonds in its high-spin excited state.[22] That is, LIESST photoexcitation leads to expansion of the host lattice, which thus creates prerequisites for expansion of the dopant copper coordination sphere.

A gradual increase of the temperature of photoswitched **2** to 70 K is accompanied by a slight decrease in $g_\parallel$, but the most pronounced jump to $g_\parallel \approx g_\parallel (T = 20$ K, dark) occurs between 70 and 80 K (Fig. 2) which again corresponds to T(LIESST) of the host lattice. The temperature evolution of $g_\perp$ is less clear, since a more pronounced gradual decrease in $g_\perp$ occurs on warming between 20-70 K. Moreover, the $g_\perp$ value at 80-90 K does not correspond exactly to that found at 20 K in the dark, where the compound also resides in its low-spin state. This indicates that the EPR spectrum of the $[Cu(terpy)_2]^{2+}$ sites in low-spin **2** is intrinsically temperature-dependent. Such behavior is typical of dynamic JT phenomena on Cu^{2+} ions.[29,38-40] This was confirmed by recording the temperature-dependent spectra of **2** between 20-70 K without illumination (Figures 2 and S4). Even more pronounced manifestations of dynamic JT effect were found for **3** (see below).

Fig. 3 shows the effect of LIESST and temperature on the EPR of the alternative Cu^{2+}-doped complex **3**. In contrast to **2**, the EPR spectrum of **3** at 20 K before illumination is assignable to a rhombically-distorted Cu^{2+} ion in an octahedral environment, with all components of g-tensor being well-resolved. Again, photoswitching of the $[Fe(bpp)_2][BF_4]_2$ host lattice results in a noticeable increase of all components of the g-tensor, being most pronounced for g_x and g_z, and less pronounced for g_y. Thus, as in **2**, the average Cu–N bond length in **3** increases upon LIESST excitation at 20 K. However, subsequent increase of the temperature results in continuous changes of the g-tensor components over the whole range of 20-90 K. As a result, the relaxation-induced discontinuities around T(LIESST) are less pronounced, but still are visible for the g_x and g_z components (Fig. 3, insets). Such a gradual dependence of $g_{x,y,z}(T)$ is assigned to strong manifestations of dynamic JT behaviour, which is also clearly visible in spectra recorded without illumination over the same temperature range (Figure S6).[41] Notably the temperature dependences $\delta g_y / \delta T$ and $\delta g_z / \delta T$, which are most sensitive to the JT fluxional process,[29,38] are essentially identical in both the irradiated and non-irradiated samples (Fig. 3, insets). That implies the thermodynamics of the JT re-orientation in $[Cu(bpp)_2]^{2+}$ are almost unaffected by the LIESST excitation in **3**, despite the expansion of its coordination sphere.

Thus, the JT nature of Cu^{2+} dopants can complicate determination of T(LIESST) by this technique due to superimposing temperature-dependent property of the dopant on top of the investigated SCO behavior. Whether this occurs (**3**) or not (**2**), depends on the ratio between T(LIESST) and the magnitude of the dopant's reorientational JT barrier.[29] The low-temperature JT fluxionality in **3** is unusual since dynamic JT behavior in most solid copper(II) compounds, including salts of $[Cu(terpy)_2]^{2+}$,[39,40] is suppressed below 50 K.[38] That allows the EPR of dopant Cu^{2+} ions to provide direct information on the spin state of a surrounding SCO lattice.
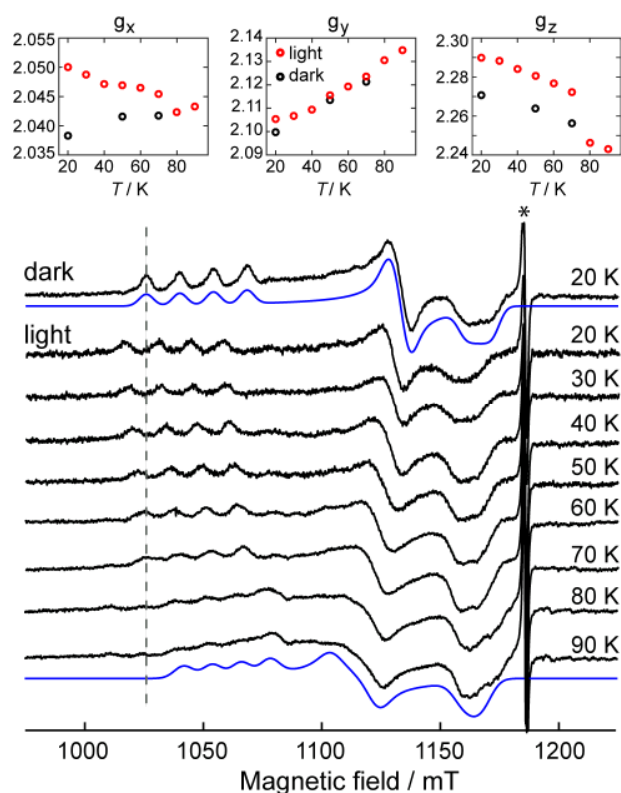

Figure 3. Q-band EPR spectra of powdered **3** dispersed in KBr. Details as in Figures 1 and 2. The upper insets show the temperature evolution of $[g_x\ g_y\ g_z]$ in the illuminated sample (red), and in the reference measurements on the same pellet without illumination (black; Figure S6).

In conclusion, we have demonstrated a potent new approach for studying LIESST phenomena by EPR of S = ½ dopant species. In this case, ca 3-4% of Co^{2+} and Cu^{2+} species were doped into the $[Fe(bpp)_2][BF_4]_2$ SCO host compound. While $3d^6$ iron(II) complexes are most studied in fundamental and applied SCO research, detection of their spin transitions by EPR is usually impractical. Their S = 0 low-spin states are clearly EPR-inactive, but their S = 2 high-spin forms are also EPR silent under most laboratory conditions, due to their fast relaxation or large zero-field splitting. Embedding dopants into such lattices has a double advantage. First, EPR spectra of both Co^{2+} and Cu^{2+} are very responsive to spin state transitions of the host material, which modulate the structure of the host lattice surrounding the dopant molecules. High-sensitivity EPR measurements on small amounts of doped compounds are therefore straightforward. Second, in perspective, allosteric switching effects in the dopant species, as in **1**, are of great additional interest. Modulation of the optical or magnetic properties of dopant species by a spin-crossover host-lattice offers a new route towards switchable multifunctional materials.

The high sensitivity and spectral selectivity that are required for detecting small dopant concentrations are both provided by EPR, but are not accessible with a traditional SQUID magnetometer for example. Therefore, we believe that this first demonstration can be a useful step forward in the design and characterisation of new SCO compounds.

ASSOCIATIED CONTENT

Supporting Information

The Supporting Information is available free of charge on the ACS Publications website at DOI: 10.1021/acs.inorgchem.xxxxxxx.

Experimental procedures, additional Figures and discussions of the EPR spectra from this work, and Tables of simulated data. (PDF)

AUTHOR INFORMATION

Corresponding Author

*E-mail: m.a.halcrow@leeds.ac.uk   (M.   A.   H.), mfedin@tomo.nsc.ru (M. V. F)

ORCID

Sergey Veber: 0000-0002-5445-3713
Malcolm Halcrow: 0000-0001-7491-9034
Matvey Fedin: 0000-0002-0537-5755

Author Contributions

All authors have given approval to the final version of the manuscript.

Notes

The authors declare no competing financial interests.

REFERENCES

(1) Spin-Crossover Materials-Properties and Applications; Halcrow, M. A., Ed.; John Wiley & Sons, Ltd.: New York, 2013; p 568.

(2) (a) Brooker, S. Spin Crossover with Thermal Hysteresis: Practicalities and Lessons Learnt. Chem. Soc. Rev. 2015, 44, 2880–2892; (b) Kumar, K. S.; Ruben, M. Emerging Trends in Spin Crossover (SCO) Based Functional Materials and Devices. Coord. Chem. Rev. 2017, 346, 176–205.

(3) Molnár, G.; Rat, S.; Salmon, L.; Nicolazzi, W.; Bousseksou, A. Spin Crossover Nanomaterials: from Fundamental Concepts to Devices. Adv. Mater. 2018, 30, 17003862/1–23.

(4) Halcrow, M. A. Structure:Function Relationships in Molecular Spin-Crossover Complexes. Chem. Soc. Rev. 2011, 40, 4119–4142.

(5) Bertoni, R.; Lorenc, M.; Tissot, A.; Boillot, M.-L.; Collet, E. Femtosecond Photoswitching Dynamics and Microsecond Thermal Conversion Driven by Laser Heating in Fe^{III} Spin-Crossover Solids. Coord. Chem. Rev. 2015, 282–283, 66–76.

(6) Unruh, D.; Homenya, P.; Kumar, M.; Sindelar, R.; Garcia, Y.; Renz, F. Spin State Switching of Metal Complexes by Visible Light or Hard X-rays. Dalton Trans. 2016, 45, 14008–14018.

(7) Hauser, A. Light-Induced Spin Crossover and the High-Spin/Low-Spin Relaxation. Top. Curr. Chem. 2004, 234, 155–198.

(8) Létard, J.-F. Photomagnetism of Iron(II) Spin Crossover Complexes – the T(LIESST) Approach. J. Mater. Chem. 2006, 16, 2550–2559.

(9) Gütlich, P.; Hauser, A.; Spiering, H. Thermal and Optical Switching of Iron(II) Complexes. Angew. Chem. Int. Ed. 1994, 33, 2024–2054.

(10) Hauser, A.; Jeftić, J.; Romstedt, H.; Hinek, R.; Spiering, H. Cooperative Phenomena and Light-Induced Bistability in Iron(II) Spin-Crossover Compounds. Coord. Chem. Rev. 1999, 190–192, 471–491.

(11) See eg (a) Paradis, N.; Chastanet, G.; Palamarciuc, T.; Rosa, P.; Varret, F.; Boukheddaden, K.; Létard, J.-F. Detailed Investigation of the Interplay Between the Thermal Decay of the Low Temperature Metastable HS State and the Thermal Hysteresis of Spin-Crossover Solids. J. Phys. Chem. C 2015, 119, 20039–20050; (b) Sylla, M. S.; Baldé, C.; Daro, N.; Desplanches, C.; Marchivie, M.; Chastanet, G. On the Effect of the Internal Pressure on the Photoinduced Spin-Crossover Behavior of [Fe$_x$M$_{1-x}$(1,10-phenanthroline)$_2$(NCS)$_2$] Solid Solutions (M = Ni^{II}, Zn^{II}, and Cd^{II}). Eur. J. Inorg. Chem. 2018, 297–304.

(12) Ozarowski, A.; McGarvey, B. R; Sarkar, A. B.; Drake, J. E. EPR Study of Manganese(II) in Two Crystalline Forms of Fe(C$_6$H$_8$N$_2$S$_2$)$_2$(NCS)$_2$ and the High-Spin-Low-Spin Transition that Occurs in Only One Form. X-Ray Structure Determination of Both Forms. Inorg. Chem. 1988, 27, 628–635 and 2560 (correction).

(13) Ozarowski, A.; McGarvey, B. R. EPR Study of Manganese(II) and Copper(II) in Single Crystals of the Spin-Crossover Complex Fe(PTZ)$_6$(BF$_4$)$_2$. Inorg. Chem. 1989, 28, 2262–2266.

(14) Kunkeler, P. J.; van Koningsbruggen, P. J.; Cornelissen, J. P.; van der Horst, A. N.; van der Kraan, A. M.; Spek, A. L.; Haasnoot, J. G.; Reedijk, J. Novel Hybrid Spin Systems of 7,7',8,8'-Tetracyanoquino-dimethane (TCNQ) Radical Anions and 4-Amino-3,5-bis(pyridin-2-yl)-1,2,4-triazole (abpt). Crystal Structure of [Fe(abpt)$_2$(TCNQ)$_2$] at 298 and 100 K, Mössbauer Spectroscopy, Magnetic Properties, and Infrared Spectroscopy of the Series [M^{II}(abpt)$_2$(TCNQ)$_2$] (M = Mn, Fe, Co, Ni, Cu, Zn). J. Am. Chem. Soc. 1996, 118, 2190–2197.

(15) (a) Rao, P. S.; Reuveni, A.; McGarvey, B. R.; Ganguli, P.; Gütlich, P. Electron Spin Resonance and Mössbauer Study of the High-Spin-Low-Spin Transition in [Fe(phen)$_2$(NCS)$_2$] and [Fe(pic)$_3$]Cl$_2$·EtOH. Inorg. Chem. 1981, 20, 204–207; (b) Doant, P. E.; McGarvey, B. R. EPR Study of Manganese(II) in Single Crystals of the Spin-Crossover Complex [Fe(2-pic)$_3$]Cl$_2$·EtOH. Evidence for Domains in Transition. Inorg. Chem. 1990, 29, 874–876.

(16) Sung, R. C. W.; McGarvey, B. R. Study of the Spin-State Transition and Phase Transformation in [Fe(bpp)$_2$][CF$_3$SO$_3$]$_2$·H$_2$O and [Fe(bpp)$_2$][BF$_4$]$_2$ Using Mn^{2+} Electron Spin Resonance. Inorg. Chem. 1999, 38, 3644–3650.

(17) (a) Daubric, H.; Cantin, C.; Thomas, C.; Kliava, J.; Létard, J.-F.; Kahn, O. Spin Transition with a Very Large Thermal Hysteresis in a Molecular Crystal: an EPR Study of Fe(PM-PEA)$_2$(NCS)$_2$. Chem. Phys. 1999, 244, 75–88; (b) Daubric, H.; Kliava, J.; Guionneau, P.; Chasseau, D.; Létard, J.-F.; Kahn, O. Spin Transition in [Fe(PM-BiA)$_2$(NCS)$_2$] Studied by the Electron Paramagnetic Resonance of the Mn^{2+} Ion. J. Phys.: Condens. Matter 2000, 12, 5481–5494.

(18) Daubric, H.; Berger, R.; Kliava, J.; Chastanet, G.; Nguyen, O.; Létard, J.-F. Light-induced Excited Spin-State Trapping of Fe^{2+} Observed by Electron Paramagnetic Resonance of Mn^{2+}. Phys. Rev. B 2002, 66, 054423/1–8.

(19) Shirai, M.; Yonemura, N.; Tayagaki, T.; Kan'no, K.; Tanaka, K. Electron Spin Resonance Study of the Photo-Induced Phase Transition in the Spin-Crossover Complex. J. Luminesc. 2001, 94–95, 529–532.

(20) Holland, J. M.; McAllister, J. A.; Lu, Z.; Kilner, C. A.; Thornton-Pett, M.; Halcrow, M. A. An Unusual Abrupt Thermal Spin-State Transition in [FeL$_2$][BF$_4$]$_2$ [L = 2,6-di(pyrazol-1-yl)pyridine]. Chem. Commun. 2001, 577–578.

(21) Carbonera, C.; Costa, J. S.; Money, V. A.; Elhaïk, J.; Howard, J. A. K.; Halcrow, M. A.; Létard, J.-F. Photomagnetic Properties of Iron(II) Spin Crossover Complexes of 2,6-Dipyrazolylpyridine and 2,6-Dipyrazolylpyrazine Ligands. Dalton Trans. 2006, 3058–3066.

(22) Money, V. A.; Evans, I. R.; Halcrow, M. A.; Goeta, A. E.; Howard, J. A. K. Light Induced Excited High Spin-State Trapping in [FeL$_2$](BF$_4$)$_2$ (L = 2,6-di(pyrazol-1-yl)pyridine). Chem. Commun. 2003, 158–159.

(23) Tovee, C. A.; Kilner, C. A.; Thomas, J. A.; Halcrow, M. A. Co-crystallising Two Functional Complex Molecules in a Terpyridine Embrace Lattice. CrystEngComm 2009, 11, 2069–2077.

(24) Halcrow, M. A.; Chastanet, G. Spin-crossover and the LIESST Effect in [Fe$_x$Co$_{1-x}$(bpp)$_2$][BF$_4$]$_2$ (1.00 ≤ x ≤ 0.77). Comparison with Bifunctional Solid Solutions of Iron and Cobalt Spin-Crossover Centers. Polyhedron 2017, 136, 5–12.

(25) Docherty, R.; Tuna, F.; Kilner, C. A.; McInnes E. J. L.; Halcrow, M. A. Suppression of the Jahn-Teller Distortion in a Six-Coordinate Copper(II) Complex by Doping it Into a Host Lattice Chem. Commun. 2012, 48, 4055–4057.

(26) Halcrow, M. A. Using One Spin-Transition to Trigger Another in Solid Solutions of Two Different Spin-Crossover Complexes. Chem. Commun. 2010, 46, 4761–4763.

(27) Chastanet, G.; Tovee, C. A.; Hyett, G.; Halcrow, M. A.; Létard, J.-F. Photomagnetic Studies on Spin-Crossover Solid Solutions Containing Two Different Metal Complexes, [Fe(1-bpp)$_2$]$_x$[M(terpy)$_2$]$_{1-x}$[BF$_4$]$_2$ (M = Ru or Co). Dalton Trans. 2012, 41, 4896–4902.

(28) The low temperature quantum mechanical tunnelling rates of cobalt(II) complexes are 10^6-10^{10} times more rapid than in analogous iron(II) compounds. Hence, photoexcited cobalt(II) compounds relax to their low-spin ground state extremely rapidly under the conditions of the LIESST experiment. Enachescu, C.; Krivokapic, I.; Zerara, M.; Real, J. A.; Amstutz, N.; Hauser, A. Optical Investigation of Spin-Crossover in Cobalt(II) Bis-Terpy Complexes. Inorg. Chim. Acta 2007, 360, 3945–3950.

(29) Halcrow, M. A. Jahn-Teller Distortions in Transition Metal Compounds, and Their Importance in Functional Molecular and Inorganic Materials. *Chem. Soc. Rev.* **2013**, *42*, 1784−1795.

(30) Analogous experiments in an X-band EPR spectrometer were less successful, affording minimal spectral changes upon irradiation of **1**-**3** under otherwise similar conditions. We attribute this to the higher spectral resolution at Q-band frequencies towards small changes in g-values; and, to the larger concentrations of EPR-active material required for X-band measurements, which were thus performed with less transparent KBr disks. Incomplete light penetration through the bulk of the sample is well-known to lead to low photoconversion efficiencies during LIESST excitation.[8]

(31) Veber, S. L.; Suturina, E. A.; Fedin, M. V.; Boldyrev, K. N.; Maryunina, K. Y.; Sagdeev, R. Z.; Ovcharenko, V. I.; Gritsan, N. P.; Bagryanskaya, E. G. FTIR Study of Thermally Induced Magnetostructural Transitions in Breathing Crystals. *Inorg. Chem.* **2015**, *54*, 3446-3455.

(32) Stoll, S.; Schweiger, A. EasySpin, a Comprehensive Software Package for Spectral Simulation and Analysis in EPR. *J. Magn. Reson.* **2006**, *178*, 42-55.

(33) Pezeshk, A.; Greenaway, F. T.; Vincow, G. Electron Paramagnetic Resonance of Low-Spin Cobalt(II) Complexes: Effect of Axial Ligation upon the Ground State. *Inorg. Chem.* **1978**, *17*, 3421-3425.

(34) Kremer, S.; Henke, W.; Reinen, D. High-Spin-Low-Spin Equilibriums of Cobalt(2+) in the Terpyridine Complexes Co(terpy)$_2$X$_2$.nH$_2$O. *Inorg. Chem.* **1982**, *21*, 3013−3022.

(35) Krivokapic, I.; Zerara, M.; Daku, M. L.; Vargas, A.; Enachescu, C.; Ambrus, C.; Tregenna-Piggott, P.; Amstutz, N.; Krausz, E.; Hauser, A. Spin-Crossover in Cobalt(II) Imine Complexes. *Coord. Chem. Rev.* **2007**, *251*, 364−378.

(36) Kilner, C. A.; Halcrow, M. A. An Unusual Discontinuity in the Thermal Spin Transition in [Co(terpy)$_2$][BF$_4$]$_2$. *Dalton Trans.* **2010**, *39*, 9008−9012.

(37) Fedin, M. V.; Veber, S. L.; Bagryanskaya, E. G.; Ovcharenko, V. I. Electron Paramagnetic Resonance of Switchable Copper-Nitroxide-Based Molecular Magnets: an Indispensable Tool for Intriguing Systems. *Coord. Chem. Rev.* **2015**, *289−290*, 341−356.

(38) See eg (a) Silver, B. L.; Getz, D. ESR of Cu^{2+}(H$_2$O)$_6$. II. A Quantitative Study of the Dynamic Jahn-Teller Effect in Copper-Doped Zinc Tutton's Salt. *J. Chem. Phys.* **1974**, *61*, 638−650; (b) Hitchman, M. A.; Maaskant, W.; van der Plas, J.; Simmons, C. J.; Stratemeier, H. Cooperative Jahn-Teller Interactions in Dynamic Copper(II) Complexes. Temperature Dependence of the Crystal Structure and EPR Spectrum of Deuterated Ammonium Copper(II) Sulfate Hexahydrate. *J. Am. Chem. Soc.* **1999**, *121*, 1488−1501; (c) Simmons, C. J.; Stratemeier, H.; Hanson, G. R.; Hitchman, M. A. Temperature Dependence of the Crystal Structure and g-Values of [(HC(Ph$_2$PO)$_3$)$_2$Cu](ClO$_4$)$_2$·2H$_2$O: Influence of Dynamic Jahn-Teller Coupling and Lattice Strain Interactions. *Inorg. Chem.* **2005**, *44*, 2753−2760.

(39) Folgado, J.-V.; Henke, W.; Allmann, R.; Stratemeier, H.; Beltrán-Porter, D.; Rojo, T.; Reinen, D. Fluxionality in Hexacoordinated Copper(II) Complexes with 2,2':6',2''-Terpyridine (Terpy) and Related Ligands: Structural and Spectroscopic Investigations. *Inorg. Chem.* **1990**, *29*, 2035−2042.

(40) Meyer, A.; Schnakenburg, G.; Glaum, R.; Schiemann, O. (Bis(terpyridine))copper(II) Tetraphenylborate: a Complex Example for the Jahn-Teller Effect. *Inorg. Chem.* **2015**, *54*, 8456-8464.

(41) Dynamic JT effects are well-known for many Cu^{2+} ions.[29,38-40] The potential energy surface of an octahedral JT distortion has three wells (local minima), each corresponding to the elongation of one of the axes of coordination octahedron. At certain temperatures the reorientational jumps become thermally activated, leading to a coalescence of corresponding spectral components. Since relative populations of the three potential wells depend on temperature according to the Boltzmann law, the spectrum shows temperature-dependent apparent g-values, as is observed for $g_{x,y}$ of **3**.